CrossMark

Magnetic, microwave absorption and structural properties of Mg–Ti added Ca–M hexaferrite nanoparticles

Ali Sharbati[1] · Gholam Reza Amiri[1]

Abstract The Mg^{2+} and Ti^{4+} ions substituted M-type $Ca(MgTi)_x Fe_{12-2x}O_{19}$ (x = 0, 0.3, 0.6, 0.9) hexagonal ferrites (x = 0, 0.3, 0.6, 0.9) were synthesized by the citrate sol–gel method. The microwave absorption, crystal structure, magnetic and morphology of the nanopowders were investigated with vector network analyzer, X-ray diffraction (XRD), vibrating sample magnetometer and transmission electron microscopy. XRD results verified the formation of M-type hexagonal structures. The particle size estimated by the Scherer formula. Results illustrated particles size is less 100 nm. The hysteresis loops showed saturation magnetization increased from 72 to 98 kA m^{-1} while coercive force decreased from 1710 to 428 Oe with Mg–Ti content. Microwave absorption properties measured by the standing-wave-ratio method in the Ku band frequency. The observations showed that $Ca(MgTi)_x Fe_{12-2x}O_{19}$ nanopowders have extraordinary microwave absorption properties. It is observed bandwidth 6.3 gigahertz (12.5–18.8 GHz with respect to − 15 dB reflection loss) for composite x = 0.6. Furthermore, the results showed a minimum reflection loss − 31.5 and − 39 dB for composites 0.6 and 0.9, respectively. It should be pointed out thickness of the composites are 1.9 mm.

1 Introduction

After World War II, with the progress of radar systems extensive research has been done on radar absorbing materials. They have been traditionally used for EMI reduction,

✉ Ali Sharbati
  sharbati_ali@yahoo.com

[1] Falavarjan Branch, Islamic Azad University, Isfahan, Iran

antenna pattern shaping and radar cross reduction. The performance of radar absorbing materials is based on the absorption of radar electromagnetic waves (and conversion to other energies). The absorption process depends on the dielectric and magnetic properties of the materials.

Utilization of radar absorbing materials founded in the 1930s shortly afterwards the advent of radar [1, 2]. The first radar absorbent material was invented in Netherlands in the 1936 [3]. This absorber has special characteristics such as low resistance and high acceptability. For absorbers, the layout requirements generally are the lowest reflectivity over the widest bandwidth. In addition to the characteristic, absorber thickness and weight are also significant attentions.

In a special assortment, absorbent materials are classified into two categories of magnetic and conductive materials [4]. Magnetic absorbers have been based on carbonyl iron and hexaferrites. These materials have absorbed in the megahertz and gigahertz bands. The performance of these materials depends on their structure and properties. By changing the physical and chemical properties of an absorber, it can exhibit various properties in different frequency bands. Absorbers come with many several shapes and structures, ranging from thick pyramidal, tile and foam structures.

Many articles have been reported to develop microwave absorbing materials with hexagonal ferrites [5–8]. In general, hexagonal ferrites are divided into several types: M, X, U, Y, Z and W [9].

In last two decade, numerous papers have been published on the studies microwave absorption and magnetic properties for M-type barium and strontium ferrites [10–12]. But rarely has been investigated microwave absorption magnetic properties calcium hexaferrite [13, 14]. According to this approach, polycrystalline $Ca(MgTi)_x Fe_{12-2x}O_{19}$ hexaferrite powders were fabricated by the citrate sol–gel method. The effects of addition Mg–Ti on microwave absorbing

properties calcium hexaferrite were studied in the frequency range of 12–20 GHz. The phase formation and morphology properties are investigated by using X-ray diffraction (XRD) and transmission electron microscopy (TEM). Meanwhile, magnetic properties (coercive force and saturation magnetization) were obtained from the hysteresis loops.

2 Experimental procedures

The calcium hexaferrites with composition $Ca(MgTi)_xFe_{12-2x}O_{19}$ were synthesized by the citrate sol–gel method. The raw materials used in the present article were calcium nitrate, iron nitrate, magnesium nitrate, titanium nitrate, citric acid and ammonia. According to the formula of $Ca(MgTi)_xFe_{12-2x}O_{19}$, stoichiometric amounts of metal nitrates were dissolved into deionized water followed by the addition of citric acid. In this research the molar ratio of metal nitrates to citric acid selected 1:1. The pH value of the solution was adjusted to 7.0 with appropriate ammonia solution. After precursor solution was slowly evaporated at 80 °C until a gel formed. Then gel was dried in an oven at 120 °C for over 1 day. Finally, the as-prepared powders were calcined at 1000 °C for 1 h to obtain the desired calcium ferrite nanoparticles.

The crystallization behavior of nanocrystalline $Ca(MgTi)_xFe_{12-2x}O_{19}$ hexaferrites were checked by X-ray diffraction with Cu K_α radiation (wavelength = 0.15405 nm) at room temperature. The magnetic properties (such as saturation magnetization (M_s) and coercive field (H_c) of nanocrystalline $Ca(MgTi)_xFe_{12-2x}O_{19}$) have been performed by using a vibrating sample magnetometer at room temperature with maximum applied magnetic fields up 12,000 Oe. Microwave absorption properties measured by standing-wave-ratio (SWR) method. The details test was reported in our previous work [15]. It should be noted that in this article absorbers thickness is 1.9 mm.

3 Results and discussions

3.1 Crystal structure

The X-ray diffraction (XRD) spectrums of $Ca(MgTi)_xFe_{12-2x}O_{19}$ (x = 0, 0.3, 0.6, 0.9) samples were presented in Fig. 1. The patterns have been indexed to hexagonal crystal system pertaining to the space group P63/mmc (No. 194), which confirms that the phase belongs to the magnetoplumbite crystal structure. Linear increase in the lattice constant by the increase of Mg–Ti ions concentration in calcium ferrites was observed. This increase is owing to the difference in cationic radii of Mg, Ti and Fe ions. Substitution of larger Mg–Ti ions with relatively smaller Fe ions
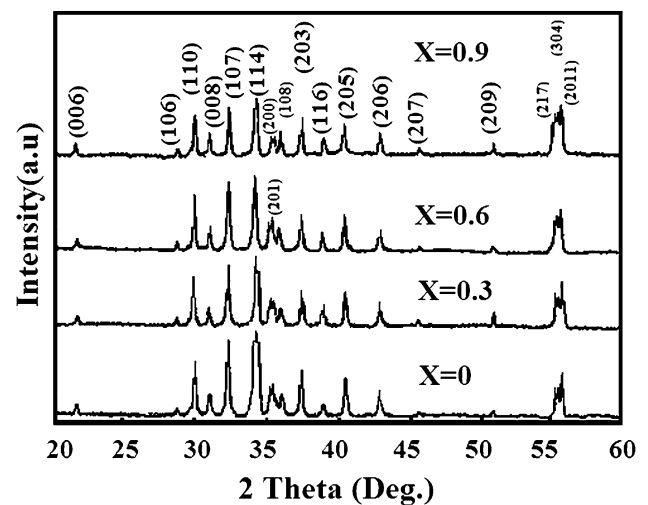

Fig. 1 XRD pattern of calcined powders at 1000 °C

Table 1 The structural parameters of $Ca(MgTi)_xFe_{12-2x}O_{19}$

x	a (nm)	c (nm)	c/a	V (nm)^3	D (nm)
0	0.5902	2.304	3.903	0.695	35
0.3	0.5899	2.303	3.904	0.694	39
0.6	0.5897	2.302	3.903	0.693	47
0.9	0.5890	2.300	3.904	0.690	68

causes the slight expansion of unit cell. Lattice constant values, calculated using the standard Eq. [16, 17], are given in Table 1. The crystallite size of samples determined by Scherrer formula [18, 19] was reported in Table 1. According to this data, the obtained powders [$Ca(MgTi)_xFe_{12-2x}O_{19}$] could be considered as nano-material, since the crystallite size of samples was < 100 nm.

Figure 2a–c illustrates TEM image of the $Ca(MgTi)_xFe_{12-2x}O_{19}$ hexaferrite samples with different Mg–Ti contents. It illustrates that the particle size is nearly symmetrical and uniform. The average particle size estimate about 39, 47, and 68 nm with x = 0.3, 0.6, and 0.9 respectively, which shows that the average particle size increases with the increase of Mg–Ti addition. The particles size in TEM images seem to be somewhat bigger than that in X-ray results, which is probably owing to the difference in resolution of the two techniques. However, it is clear that the particle size is much below 100 nm.

3.2 Magnetic properties

The M–H loops for $Ca(MgTi)_xFe_{12-2x}O_{19}$ with x = 0.0, 0.3, 0.6, and 0.9 M-type hexagonal ferrites are shown in Fig. 3. All the samples exhibit hysteresis behavior, indicative of
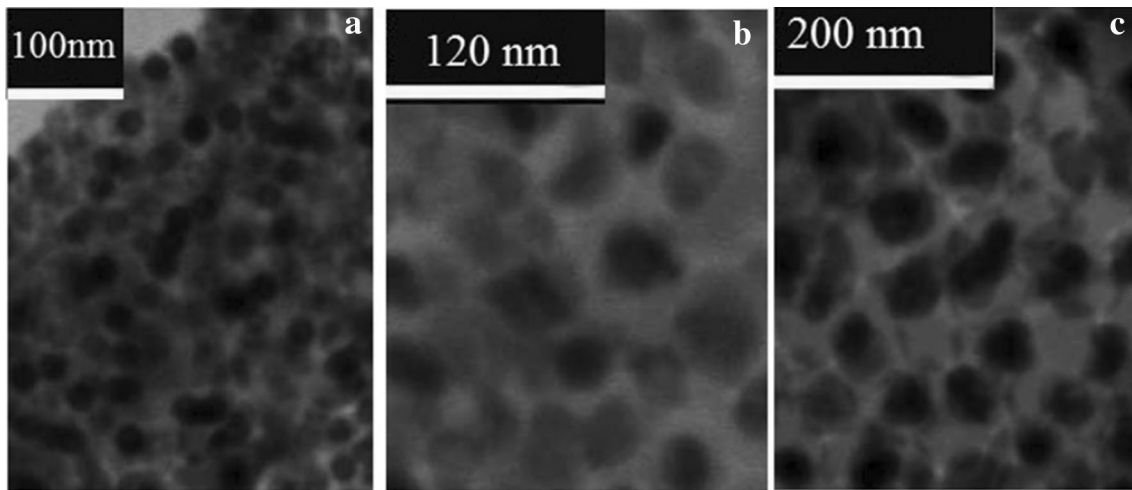
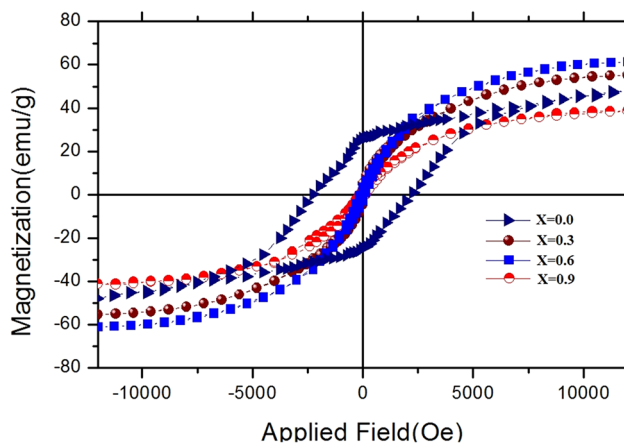**Fig. 2** TEM micrographs of prepared powders: **a** x = 0.3, **b** x = 0.6, **c** x = 0.9

Fig. 3 Room temperature hysteresis loops of x = 0, x = 0.3, x = 0.6 and x = 0.9

ferrimagnetism. The values of the saturation magnetization (M_s) and coercivity (H_c) are presented in Table 1.

Figure 3 shows that M_s increases at low substitution, reaching a maximum at x = 0.6, and then decreases. Given the Gorter model [20], the 24 Fe^{3+} ions of M-type hexaferrite are distributed on five different crystallographic sites: three up-spin sites (2a, 12k and 2b) and two down-spin sites ($4f_1$ and $4f_2$) along the c axis. The Mg–Ti substitution in different Fe^{3+} sites makes contribution to the magnetic properties of the calcium ferrite.

Both the doped ions (Ti^{4+} and Mg^{2+}) are nonmagnetic with their spins in the downward direction [21, 22]. As they replace iron ions at the tetrahedral ($4f_1$) sites and the net spin of the Fe^{3+} ions in the upward direction increases, the total magnetic moment increases; and so does the saturation magnetization.

The decrease in saturation magnetization above x = 0.6 is due to the larger amount of nonmagnetic ions which are responsible for the weakening of the exchange interactions [23].

In general, the results show that substitutions lead to a decrease in H_c through the reduction of the magnetocrystalline anisotropy of calcium ferrite. It is observed that the undoped sample possesses the largest coercive force (H_c), the largest hysteresis loop area and the highest Ca. The former two may lead the larger loss. The H_c of pure calcium ferrite is very high, which is due to strong uniaxial anisotropy along the c-axis of M-hexaferrite. On the other hand, Mg and Ti substitution led to a rapid decrease in H_c. The result is attributed to the reduction in the crystal anisotropy field due to the change of the easy-axis of magnetization from the c-axis to the basal plane [24, 25]. It should be noted that it is well known fact that coercive force is heavily dependent upon grain size and saturation magnetization [26–29].

3.3 Attenuation properties

For a microwave absorbing layer terminated by metal plate, the normalized input impedance at the absorber surface (Z_{in}) is given by (1) [30]:

$$Z_{in} = \sqrt{\frac{\mu_r}{\varepsilon_r}} \tanh \left[j\frac{2\pi}{c} \sqrt{\mu_r \varepsilon_r} fd \right] \tag{1}$$

where Z_{in} is the impedance of the composites, Z_0 is the intrinsic impedance of free space, c is the light velocity, d is the thickness of composite, f is the frequency of the incident EM wave, μ is the complex permeability and ε is the complex permittivity. When EM wave propagating through a free-space is incident upon a semi-infinite dielectric or magnetic

dielectric material of impedance Z_{in}, a partial reflection occurs. The reflection loss (R.L.) could be described as [31]

$$RL(dB) = 20 \log \left| \frac{Z_{in} - 1}{Z_{in} + 1} \right| \qquad (2)$$

The transmission losses of $Ca(MgTi)_x Fe_{12-2x} O_{19}$ ferrite (70 wt%)–polymer (30 wt%) composites with 1.9 mm thickness are depicted in Fig. 4. For sample "x = 0", the effective reflection loss was not observed in the 12–20 GHz regions because of the high natural resonance frequency of this sample. As shown in figure, the minimum reflection coefficient is about -30 and -31.5 dB for the composites of $Ca(MgTi)_{0.3} Fe_{11.4} O_{19}$ and $Ca(MgTi)_{0.6} Fe_{10.8} O_{19}$. Also, it can be seen that sample "x = 0.6" has another peak at 14.7 GHz. In addition to, results indicate minimum RL of $Ca(MgTi)_{0.9} Fe_{10.2} O_{19}$ is -39 dB at frequency of 16.6 GHz. Moreover, band widths that covered these composites (with respect to -15 dB reflection loss) are 1.7 GHz (for x = 0.3), 6.2 GHz (for x = 0.6) and 4.7 GHz (for x = 0.9). It should be noted that for composite "x = 0", the effective reflection loss was not found in frequency range from 12 to 20 GHz. Also, it is evident that the position of minimum reflection loss peak is moving towards the higher frequency region with the increase $Mg^{2+} Ti^{4+}$ content.

According to the ferromagnetic resonance theory [32], the resonance frequency (f_r) in hexagonal crystal is closely related with the magnetic properties which is given by:

$$f_r(1 - \mu_i) = \frac{1}{3\pi\mu_0} \gamma M_s \left(\frac{1}{2} \sqrt{\frac{H_{a1}}{H_{a2}}} + \frac{1}{2} \sqrt{\frac{H_{a2}}{H_{a1}}} \right) \qquad (3)$$

where μ_i is initial permeability, μ_0 is permeability of vacuum and γ is gyromagnetic constant. H_{a1} is the anisotropy field

for the magnetization rotation in the easy plane and H_{a2} is that for rotation out of the plane. In random polycrystals, it is difficult to determine the H_{a1} and H_{a2}. If the coercivity can be taken as a degree of the anisotropy field, the resonance frequency is considered to be proportional to the saturated magnetization (M_s) and the coercivity. The present result is quite well consistent with the ferromagnetic resonance theory.

It should be pointed out a well microwave absorption material need to have low reflection loss, wide absorption bandwidth, and low matching thickness. It is, however, difficult to obtain all these characteristics in one single absorber. However, in the present study, the reflection coefficient decreased with the increasing applied field frequency as well as with the increasing Mg–Ti contents. Hence, the synthesized powders can be considered as potential candidates for high-frequency applications such as stealth technology, anechoic chambers, camouflaging, and attenuations of electromagnetic interference.

4 Conclusions

In this research, Ca–M-type hexaferrite magnetic nanoparticles were successfully synthesized by the citrate sol–gel method. The structure of the samples was investigated by XRD and TEM. The X-ray diffraction results showed the formation of hexagonal structure. The TEM images illustrated that the morphology of the synthesized ferrites nanoparticles are approximately spherical in shape with size distribution between 30 and 40 nm which is in good agreement with the size achieved from XRD. From hysteresis loops it was found that with the increase of MgTi concentration, saturation magnetization and coercive force are decreased. The microwave absorption properties of ferrite-resin (70–30 wt%) calculated by using a SWR method. The present study exhibited that the prepared group of Mg and Ti doped Ca–M-hexaferrite composites include lossy materials which could be interestingly applied in the design of new microwave absorbing structures particularly in the Ku band frequency.
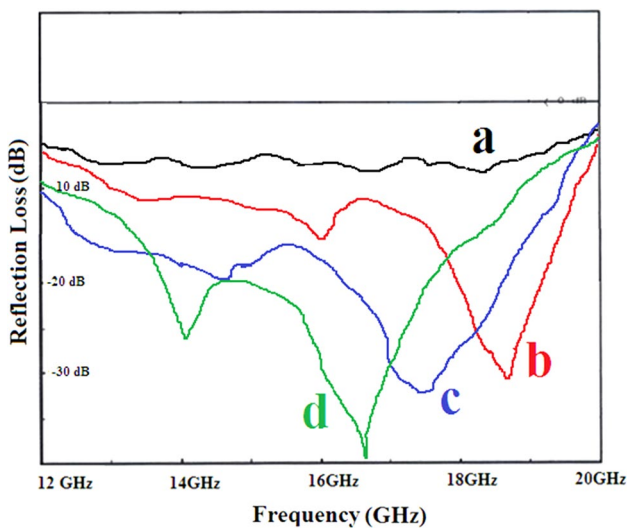
Fig. 4 Absorption characteristics of the composite: **a** x = 0, **b** x = 0.3, **c** x = 0.6 and **d** x = 0.9

References

1. J.A. Walker et al., J. Polym. Sci. A **26**, 1285 (1988)
2. W.H. Emerson, IEEE Trans. Antennas Propag. **21**, 484 (1973)
3. N.V. Machinerieen, FR Patent. 802728 (1936)
4. X. Chen et al., J. Mater. Sci. **27**, 10045 (2016)
5. A. Sharbati et al., J. Mater. Sci. **25**, 244 (2014)
6. N. Chen et al., Mater. Sci. Eng. B **256**, 139 (2007)
7. J. Qiu et al., Powder Technol. **154**, 116 (2005)
8. J. Singh et al., J. Alloys Compd. **695**, 792 (2017)
9. A. Sharbati et al., Dig. J. Nanomater. Biostruct. **187**, 6 (2011)
10. C. Singh et al., J. Alloys Compd. **683**, 302 (2016)
11. S.B. Narang et al., JMMM, **405**, 17 (2016)
12. S.V. Trukhanov et al., JMMM **442**, 300 (2017)
13. V.A.D. Silva et al., J. Aerosp. Technol. Manag. **1**, 255 (2009)
14. S.B. Narang et al., J. Ceram. Process. Res. **7**, 113 (2006)
15. A. Sharbati et al., Solid State Commun. **152**, 199 (2012)
16. M. Lakshmi et al., J. Nanostruct. Chem. **5**, 365 (2015)
17. G. Aravind et al., J. Nanostruct. Chem. **5**, 77 (2015)
18. S. Abedini Khorrami et al., Int. J. Nano Dimension **3**, 191 (2013)
19. L. Kumar et al., Int. Nano Lett. **3**, 1 (2013)
20. K. Samikannu et al., Mater. Sci. Appl. **2**, 638 (2011)
21. A. Sharbati et al, Solid State Commun. **150**, 2218 (2010)
22. J. Li, et al, Mater. Res. Express **2**, 046104 (2015)
23. M. Iqbal et al., Scr. Mater. **57**, 1093 (2007)
24. Y.J. Kim,et al, IEEE Trans. Magn. **38**, 3108 (2002)
25. S.P. Gairola et al., J. Integr. Ferroelectr. **119**, 151 (2009)
26. G. Allaedini et al., Int. Nano Lett. **5**, 183 (2015)
27. R.H. Kadam et al., Int. Nano Lett. **2**, 1 (2012)
28. G. Nabiyouni et al., J. Nanostruct. **2**, 527 (2013)
29. G. Nabiyouni et al., J. Nanostruct. **7**, 77 (2017)
30. P. Mehdizadeh et al., J. Nanostruct. **6**, 140 (2016)
31. F. Azizi et al., J. Nanostruct. **5**, 345 (2015)
32. H. Shin Cho et al., IEEE Trans. Magn. **35**, 3151 (1999)